

Detecting Microscopic Black Holes with Neutrino Telescopes

Jaime Alvarez-Muñiz,¹ Jonathan L. Feng,^{2,3} Francis Halzen,⁴ Tao Han,⁴ and Dan Hooper⁴

¹*Bartol Research Institute, University of Delaware, Newark, DE 19716*

²*Center for Theoretical Physics, Massachusetts
Institute of Technology, Cambridge, MA 02139*

³*Department of Physics and Astronomy,
University of California, Irvine, CA 92697*

⁴*Department of Physics, University of Wisconsin,
1150 University Avenue, Madison, WI 53706*

Abstract

If spacetime has more than four dimensions, ultra-high energy cosmic rays may create microscopic black holes. Black holes created by cosmic neutrinos in the Earth will evaporate, and the resulting hadronic showers, muons, and taus may be detected in neutrino telescopes below the Earth's surface. We simulate such events in detail and consider black hole cross sections with and without an exponential suppression factor. We find observable rates in both cases: for conservative cosmogenic neutrino fluxes, several black hole events per year are observable at the IceCube detector; for fluxes at the Waxman-Bahcall bound, tens of events per year are possible. We also present zenith angle and energy distributions for all three channels. The ability of neutrino telescopes to differentiate hadrons, muons, and possibly taus, and to measure these distributions provides a unique opportunity to identify black holes, to experimentally constrain the form of black hole production cross sections, and to study Hawking evaporation.

I. INTRODUCTION

The possibility that we live in $D = 4 + n > 4$ spacetime dimensions has profound implications. In particular, if gravity propagates in these extra dimensions, the fundamental Planck scale M_D at which gravity becomes comparable in strength to other forces may be far below $M_4 \sim 10^{19}$ GeV, leading to a host of potential signatures for high energy physics [1].

Among the most striking consequences of low-scale gravity is the possibility of black hole creation in high-energy particle collisions [2, 3, 4, 5, 6, 7, 8, 9]. In most gravitational processes, such as those involving graviton emission and exchange, analyses rely on a perturbative description that breaks down for center-of-mass energies of M_D and above. In contrast, black hole properties are best understood for energies above M_D , where semi-classical and thermodynamic descriptions become increasingly valid [10]. In principle, then, black holes provide a robust probe of extra dimensions and low-scale gravity, as long as particle collisions with center-of-mass energies above $M_D \sim 1$ TeV are available.

Nature provides interactions at the necessary energies in the form of cosmic rays with energies above 10^{10} GeV. In collisions with nucleons, these cosmic rays probe center-of-mass energies exceeding 100 TeV, beyond both current man-made colliders and those of the foreseeable future. Cosmic neutrinos may create black holes deep in the Earth's atmosphere, resulting in spectacular signals of giant air showers in ground arrays and fluorescence detectors [11, 12, 13, 14, 15]. With a handful of events, standard model (SM) and most alternative explanations may be excluded [11, 15] by comparison with rates for Earth-skimming neutrinos [16, 17, 18], and with more events, black holes may be identified through their shower characteristics [12]. Bounds have been derived [14, 15] from the absence of such showers in current data from Fly's Eye [19] and AGASA [20]. For conservative fluxes and the geometric black hole cross section, the AGASA data require $M_D \gtrsim 1.3 - 1.8$ TeV for $n \geq 4$, the most stringent constraint to date [15]. At the same time, the Auger Observatory, scheduled for completion by 2004, may observe tens of black hole events per year [11, 14, 15]. Related phenomena related to p -brane production may also be observed in cosmic rays [21, 22].

Here we examine the possibility of detecting and studying black holes produced by cosmic neutrinos in neutrino telescopes. Several large-scale neutrino telescope projects are underway, including IceCube [23] in the Antarctic ice, and ANTARES [24] and NESTOR [25] in the Mediterranean. Among the many possible black hole signatures, such detectors are most sensitive to contained hadronic showers and through-going muons and taus from the evaporation of black holes produced in the Earth's crust. The possibility of black hole detection in neutrino telescopes has recently been studied in Ref. [26]; where possible, we will compare our results to those of Ref. [26] below. For a preliminary study, see also Ref. [27].

For TeV-scale gravity and conservative flux assumptions, we find that IceCube could detect several black holes per year. These rates may be enhanced by larger fluxes, and observable rates are possible even given a postulated exponential suppression factor in the black hole cross section [28, 29]. The relative event rates in the three channels may differ from the SM, and the energy and angle distributions of black hole events are also distinctive. These will not only help identify black holes, but may also constrain parameters such as n and M_D , and determine if suppression factors in the cross section are present or absent. The search for black holes in neutrino telescopes therefore complements black hole searches in other cosmic ray detectors, as well as searches for the effects of perturbative gravity processes at center-of-mass energies below M_D [30, 31, 32, 33].

II. BLACK HOLE PRODUCTION AND EVAPORATION

In $D = 4 + n$ dimensions, gravity is described by the Einstein action

$$S_E = \frac{1}{8\pi G_D} \int d^{4+n}x \sqrt{-g} \frac{1}{2} \mathcal{R} , \quad (1)$$

where G_D is the D -dimensional Newton's constant. To define the fundamental Planck scale M_D , we adopt the convention

$$\frac{1}{8\pi G_D} = \frac{M_D^{2+n}}{(2\pi)^n} . \quad (2)$$

In the most straightforward scenarios [1] with flat extra dimensions of equal length, TeV-scale gravity is excluded for $n = 1$ by solar system tests of Newtonian gravity. Astrophysical bounds [34] on supernova cooling and neutron star heating provide the most stringent bounds for $n = 2$ ($M_D \gtrsim 600$ TeV) and $n = 3$ ($M_D \gtrsim 10$ TeV). For $n \geq 4$, the most stringent bounds are from collider searches for perturbative graviton effects [35, 36, 37] and cosmic ray bounds on black hole production [14, 15, 19, 20]. These constraints are each subject to a variety of theoretical assumptions (for a comparison and discussion, see, *e.g.*, Ref. [15]), but the most stringent of these require roughly $M_D \gtrsim 1$ TeV.

To determine event rates for neutrino telescopes, we must first model black hole production and evaporation. For production by cosmic neutrinos, we follow the analysis of Ref. [11]. Black holes produced in parton collisions are typically far smaller than the length scales of the extra dimensions. These black holes are then well-approximated by $(4+n)$ -dimensional solutions. The Schwarzschild radius for a $(4+n)$ -dimensional black hole with mass M_{BH} and vanishing charge and angular momentum is [38]

$$r_s(M_{\text{BH}}^2) = \frac{1}{M_D} \left[\frac{M_{\text{BH}}}{M_D} \right]^{\frac{1}{1+n}} \left[\frac{2^n \pi^{\frac{n-3}{2}} \Gamma\left(\frac{3+n}{2}\right)}{2+n} \right]^{\frac{1}{1+n}} . \quad (3)$$

We assume that two partons i and j with center-of-mass energy $\sqrt{\hat{s}}$ form a black hole of mass $M_{\text{BH}} = \sqrt{\hat{s}}$ when they pass within a distance $r_s(\hat{s})$, leading to a geometric cross section of [5, 8, 9]

$$\hat{\sigma}(ij \rightarrow \text{BH})(\hat{s}) = \pi r_s^2(\hat{s}) . \quad (4)$$

Evidence from analyses of axisymmetric [39] and off-axis [40] classical collisions, an analysis in a simple model framework [41], and a string calculation [42] suggests that this picture is valid semi-classically and is not subject to large corrections [43]. Modifications for non-vanishing angular momentum and spinning black holes have also been found to be small [15]. However, Voloshin has argued [28, 29] that the cross section could be suppressed by the factor e^{-I} , where the action is

$$I = \frac{S}{n+1} = \frac{4\pi M_{\text{BH}} r_s}{(n+1)(n+2)} , \quad (5)$$

with S the black hole entropy. This implies vanishing cross sections in the classical limit, contrary to the evidence noted above. To explore the impact of modifications to the black hole production cross section, however, we consider cases both with and without this suppression.

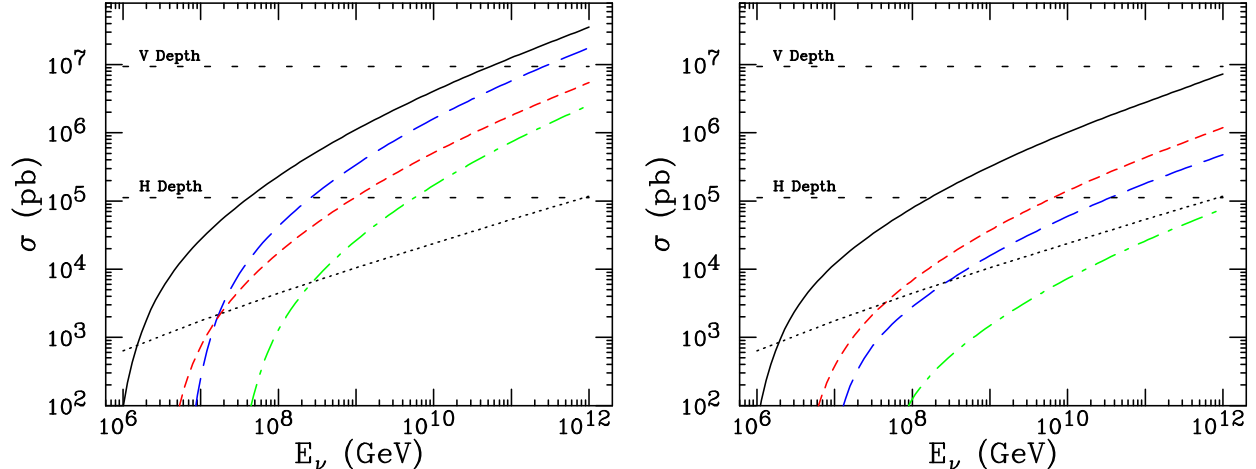


FIG. 1: Cross sections $\sigma(\nu N \rightarrow \text{BH})$ for $n = 6$ and $(M_D, x_{\min}) = (1 \text{ TeV}, 1)$ (solid), $(1 \text{ TeV}, 3)$ (long dash), $(2 \text{ TeV}, 1)$ (short dash), $(2 \text{ TeV}, 3)$ (dot-dash), and parton cross sections πr_s^2 (left) and $\pi r_s^2 e^{-I}$ (right). The dotted curve is the SM cross section $\sigma(\nu N \rightarrow \ell X)$. The horizontal lines are the cross sections corresponding to interaction lengths equal to the vertical and horizontal depths of IceCube. (See text.)

The neutrino-nucleon scattering cross section is then [11]

$$\sigma(\nu N \rightarrow \text{BH}) = \sum_i \int_{(x_{\min} M_D)^2/s}^1 dx \hat{\sigma}_i(xs) f_i(x, Q), \quad (6)$$

where

$$x_{\min} \equiv M_{\text{BH}}^{\min}/M_D \gtrsim 1 \quad (7)$$

parameterizes the minimal black hole mass for which we expect a semi-classical description to be valid, $s = 2m_N E_\nu$, the sum is over all partons i , and f_i are the parton distribution functions. The cross section is highly insensitive to choice of momentum transfer [11]; *e.g.*, the choices $Q = M_{\text{BH}}$ [9] and $Q = r_s^{-1}$ [13], lead to cross section differences of only 10% to 20%. These cross sections are typically also insensitive to uncertainties at low x . For example, even extremely high energy neutrinos with $E_\nu \sim 10^{10}$ GeV probe only $x \gtrsim (1 \text{ TeV})^2/10^{10} \text{ GeV}^2 \approx 10^{-4}$, within the range of validity of the CTEQ5 parton distribution functions we use [44].

Cross sections for black hole production by cosmic neutrinos are given in Fig. 1. The SM cross section for $\nu N \rightarrow \ell X$ is included for comparison (dotted curve). As a result of the sum over all partons and the lack of suppression from small perturbative couplings, the black hole cross section may exceed SM interaction rates by two or more orders of magnitude.

Note that in our conventions, the cross section rises for increasing n and fixed M_D . In conventions where the fundamental Planck scale is taken to be M_* with

$$\frac{1}{G_D} = M_*^{2+n}, \quad (8)$$

this behavior is reversed: the cross section decreases for increasing n and fixed M_* [11]. The dependence of the cross section on n for fixed Planck scale is convention-dependent and unphysical; we have adopted the M_D convention to simplify comparison with existing collider bounds.

Assuming a constant density of 1.0 g/cm^3 for the Earth's surface near the detector, as is valid for IceCube, the neutrino's interaction length in Earth is

$$L = 1.7 \times 10^7 \text{ km} \left(\frac{\text{pb}}{\sigma} \right) . \quad (9)$$

The center of IceCube is at a depth of roughly 1.8 km. A neutrino reaching this point horizontally passes through 150 km of Earth. The cross sections corresponding to neutrino interaction lengths equal to these two lengths, that is, the horizontal and vertical depths of IceCube, are also given in Fig. 1. We see that for the geometric cross section, $M_D \sim 1 \text{ TeV}$, and neutrino energies $E_\nu \sim 10^9 \text{ GeV}$ where the cosmogenic flux peaks (see Sec. III), black hole production increases the probability of conversion in down-going neutrinos without increasing the cross section so much that vertical neutrinos are shadowed by the Earth. We therefore expect significantly enhanced rates in neutrino telescopes. (On the other hand, the upgoing event rates will be even more suppressed.) For the exponentially suppressed cross section, a similar enhancement is also possible for $M_D = 1$ to 2 TeV .

Once produced, these tiny black holes evaporate with rest lifetime of order $\text{TeV}^{-1} \sim 10^{-27} \text{ s}$. Even though highly boosted, they decay before accreting matter. They evaporate in a thermal distribution with temperature $T_H = (1+n)/(4\pi r_s)$ [10, 38] and average multiplicity [8, 9]

$$\langle N \rangle \approx \frac{M_{\text{BH}}}{2T_H} = \frac{2\pi}{1+n} \left[\frac{M_{\text{BH}}}{M_D} \right]^{\frac{2+n}{1+n}} \left[\frac{2^n \pi^{\frac{n-3}{2}} \Gamma\left(\frac{3+n}{2}\right)}{2+n} \right]^{\frac{1}{1+n}} . \quad (10)$$

Neglecting particle masses, the decay products are distributed according to the number of degrees of freedom [6]: quarks (72), gluons (16), charged leptons (12), neutrinos (6), W and Z bosons (9), photons (2), Higgs bosons (1), and gravitons (2). We neglect the possibility of other low mass degrees of freedom, such as right-handed neutrinos and supersymmetric particles. About 75% of the black hole's energy is radiated in hadronic degrees of freedom, while the probability of any given decay particle being a muon (or a tau) is approximately 3%.

As through-going muons and taus will be a promising signal in neutrino telescopes, the typical multiplicity of black hole decays is of great importance. To quantify this, we define a weighted multiplicity

$$\bar{N} = \frac{1}{\sigma} \sum_i \int_{(x_{\min} M_D)^2/s}^1 dx \langle N \rangle \hat{\sigma}_i(xs) f_i(x, Q) , \quad (11)$$

where σ is given in Eq. (6), and $\langle N \rangle$ is as in Eq. (10) with $M_{\text{BH}}^2 = xs$. The weighted multiplicity \bar{N} is given in Fig. 2 for various cases with $n = 6$ and $M_D = 1 \text{ TeV}$. For the geometric black hole cross section, these multiplicities may be substantially enhanced for lower n ; for the exponentially suppressed cross section, the dependence on n is slight. We find that $\bar{N} \sim \mathcal{O}(10)$ is possible for ultra-high energy neutrinos. Note that while raising x_{\min} and including the exponential suppression factor both suppress the total cross section, they have opposite effects on \bar{N} : raising x_{\min} eliminates events with relatively low multiplicity, and so raises \bar{N} , while the exponential suppression is largest for events with large M_{BH} and large multiplicity, and so suppresses \bar{N} .

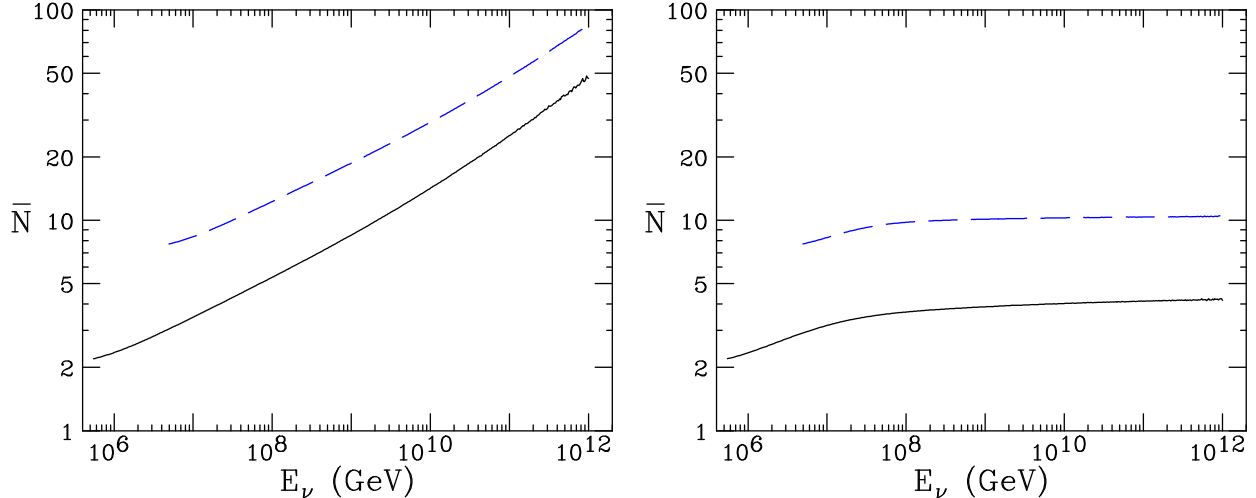


FIG. 2: Weighted multiplicities \bar{N} for $n = 6$, $M_D = 1$ TeV, and $x_{\min} = 1$ (solid) and 3 (long dash), and parton cross sections πr_s^2 (left) and $\pi r_s^2 e^{-I}$ (right).

III. ASTROPHYSICAL SOURCES OF ULTRA-HIGH ENERGY NEUTRINOS

Observations of black hole formation and decay are most easily made with neutrino fluxes that are large near or above the EeV scale. Several such sources have been proposed in the literature. While a detailed discussion of these sources is beyond the scope of this paper, we briefly describe here a few of them, including those used in our study.

First, neutrinos are almost certainly produced through pion decays in the scattering of protons off the cosmic microwave background, $p\gamma_{\text{CMB}} \rightarrow n\pi^+$ [45]. This cosmogenic flux is subject to a number of quantitative uncertainties, including cosmological source evolution. As representative fluxes, we consider the recent results presented in Fig. 4 of Ref. [46]. These fluxes are shown in Fig. 3.

Second, gamma ray bursts have also been considered as a possible source of the highest energy cosmic rays. If this is the case, Fermi accelerated protons from shocks will generate extremely high energy neutrinos with energy spectrum $d\Phi_\nu/dE_\nu \propto E_\nu^{-2}$ [47, 48, 49, 50]. This neutrino flux, as well as those from other compact sources, such as active galactic nuclei, is limited by the Waxman-Bahcall (WB) bound [51]. This constraint is valid for all astrophysical neutrino sources that are optically thin to $p\gamma$ and pp interactions. We consider a conservative estimate of this bound, $E_\nu^2 d\Phi_\nu/dE_\nu = 1 \times 10^{-8} \text{ cm}^{-2} \text{ s}^{-1} \text{ sr}^{-1}$ [51], where here $\nu = \nu_e, \nu_\mu, \bar{\nu}_\mu$. This flux is also shown in Fig. 3. It is approximately equal to the cosmogenic flux for $E_\nu \sim 10^{10}$ GeV, but is much larger for lower (and higher) energies.

Third, if the highest energy cosmic rays observed are generated by the annihilation of superheavy dark matter particles or from the decay of topological defects, neutrinos will also be produced. Such fluxes have been described in Refs. [52, 53, 54, 55]. We will not discuss these sources further, but note that they may predict large neutrino fluxes at extremely high energies, enhancing the results given below.

In propagating to the Earth, the neutrino fluxes of Fig. 3 will mix [56]. Given the solutions preferred by neutrino oscillation experiments and the enormous distances traveled, we take the neutrinos that reach the Earth to be in the ratio $\nu_e : \nu_\mu : \nu_\tau = 1 : 1 : 1$ and similarly for anti-neutrinos.

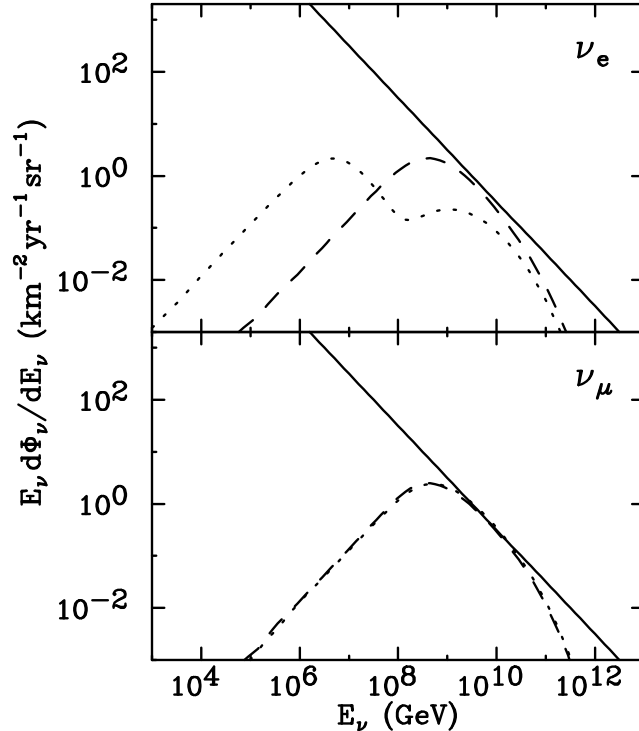


FIG. 3: Representative fluxes: cosmogenic ν (dashed) and $\bar{\nu}$ (dotted) [46] and the Waxman-Bahcall flux $\Phi_{\nu_e} = \Phi_{\nu_\mu} = \Phi_{\bar{\nu}_\mu}$ (solid) [51].

IV. EVENT SIMULATION

With regard to signals at neutrino telescopes, black hole evaporation products may be divided into three categories: showers (hadronic and electromagnetic), muons, and taus. Black holes also decay to neutrinos, but we neglect this flux in this work.

The ranges of typical hadronic and electromagnetic showers are much less than the linear dimension of large-scale neutrino telescopes, and so, to first approximation, only contained showers from black holes produced inside the detector may be detected. The backgrounds for showers from black hole evaporation consist of hadronic showers from neutral and charged current neutrino events and electromagnetic showers from charged current electron neutrino events. At IceCube, hadronic shower energies should be measurable with an accuracy of about 30%.

In contrast to showers, at the typical energies of black hole events, muons travel several kilometers before losing a decade of energy. The dominant signal is therefore through-going muons. IceCube can measure the energy and direction of any observed muon. The angular resolution is about $2^\circ - 3^\circ$ while the energy resolution is approximately a factor of three. Signal and background muons may therefore be differentiated with an energy cutoff. As we will see, for down-going muons with energy above 500 TeV to 1 PeV, the black hole signal may be well above the SM background from atmospheric neutrinos. Note that for black holes produced sufficiently near the detector, muon events may be obscured by showers. This occurrence is rare, however, and we ignore this possibility below.

At high energies, when tau decay is sufficiently time dilated, taus have ranges as large or larger than muons, and so the dominant tau signal is from through-going taus. These

events have a characteristic signature consisting of a “clean” track, *i.e.*, a track without much energy lost through low energy cascades. We will consider all events in which a tau track passes through the detector. Taus can be differentiated from muons by the cleanliness of their tracks or through their decays in the detector leading to “lollipop” events [57], described later in this paper. We assume that taus and muons are distinguishable at all energies, although it will be difficult to distinguish a slow muon of energy $\lesssim 200$ GeV from a very high energy tau, as they can both generate clean, through-going tracks in the detector.

Very massive black holes with large multiplicity decays may evaporate to several muons (or taus). However, these travel in coincidence through the detector. Their angular spread is only $\Delta\theta \sim T_H \langle N \rangle / E_\nu$, much less than a degree, and so cannot be resolved with large Cerenkov detectors such as IceCube. Spectacular multi-lepton signatures are therefore not possible. Note, however, that more massive black holes are easier to detect, as they produce leptons with greater energy, which travel further before dropping below the cutoff energy.

To evaluate black hole detection prospects, it is essential to determine, in a unified framework, both the SM background and the black hole event rate. We now describe both of these calculations.

A. Standard Model Events

1. Showers

In the SM, a general expression for the total number of shower events in an underground detector is

$$N_{\text{sh}} = \sum_{i,j} 2\pi AT \int d\cos\theta_z \int dE_{\nu_i} \frac{d\Phi_{\nu_i}}{dE_{\nu_i}}(E_{\nu_i}) P_{\text{surv}} \\ \times \int_{y_{\text{min}}^{i,j}}^{y_{\text{max}}^{i,j}} dy \frac{1}{\sigma_{\text{SM}}^j(E_{\nu_i})} \frac{d\sigma_{\text{SM}}^j}{dy}(E_{\nu_i}) P_{\text{int}} , \quad (12)$$

where θ_z is the zenith angle ($\theta_z = 0$ is vertically downward), and the sums are over neutrino (and anti-neutrino) flavors $i = e, \mu, \tau$ and interactions $j = \text{CC}$ (charged current) and NC (neutral current). A is the detector’s cross sectional area with respect to the ν flux, T is its observation time, and $d\Phi_{\nu_i}/dE_{\nu_i}$ is the differential neutrino flux that reaches the Earth. For $i = \tau$, Eq. (12) is modified to include the effects of regeneration, as discussed below.

P_{surv} is the probability that a neutrino survives to reach the detector. It is given by

$$P_{\text{surv}} \equiv \exp[-X(\theta_z)\sigma_{\text{SM}}^{\text{tot}}(E_{\nu_i})N_A] , \quad (13)$$

where $N_A \simeq 6.022 \times 10^{23} \text{ g}^{-1}$, and the total neutrino interaction cross section is

$$\sigma_{\text{SM}}^{\text{tot}} = \sigma^{\text{CC}} + \sigma^{\text{NC}} . \quad (14)$$

Note that this is conservative, as it neglects the possibility of a neutrino interacting through a NC interaction and continuing on to create a contained shower. $X(\theta_z)$ is the column density of material the neutrino must traverse to reach the detector with zenith angle θ_z . It depends on the depth of the detector and is given by

$$X(\theta_z) = \int_{\theta_z} \rho(r(\theta_z, l)) dl , \quad (15)$$

the path length along direction θ_z weighted by the Earth's density ρ at distance r from the Earth's center. For the Earth's density profile, we adopt the piecewise continuous density function $\rho(r)$ of the Preliminary Earth Model [58].

P_{int} is the probability that the neutrino interacts in the detector. It is given by

$$P_{\text{int}} = 1 - \exp \left[-\frac{L}{L_{\text{SM}}^j(E_{\nu_i})} \right], \quad (16)$$

where, for showers, L is the linear dimension of the detector, and $L_{\text{SM}}^j(E_{\nu_i})$ is the mean free path for neutrino interaction of type j . For realistic detectors, $L \ll L_{\text{SM}}^j(E_{\nu_i})$, and so $P_{\text{int}} \approx L/L_{\text{SM}}^j(E_{\nu_i})$. To an excellent approximation, then, the shower event rate scales linearly with detector volume $V = AL$, and we present results in units of events/volume/time.

Finally, the inelasticity parameter y is the fraction of the neutrino energy carried away in hadrons. The limits of integration are determined by the interaction type and neutrino flavor. For NC ν_e interactions and all ν_μ and ν_τ interactions, $y_{\text{max}} = 1$ and $y_{\text{min}} = E_{\text{sh}}^{\text{thr}}/E_\nu$, where $E_{\text{sh}}^{\text{thr}}$ is the threshold energy for shower detection. For CC ν_e interactions, the outgoing electron also showers, and so $y_{\text{max}} = 1$ and $y_{\text{min}} = 0$.

2. Muons

Energetic through-going muons are produced only by ν_μ CC interactions. For a muon to be detected, it must reach the detector with energy above some threshold E_μ^{thr} . The expression of Eq. (12) then also describes the number of muon events with P_{surv} as before, but with

$$P_{\text{int}} = 1 - \exp \left[-\frac{R_\mu}{L_{\text{SM}}^{\text{CC}}(E_{\nu_\mu})} \right], \quad (17)$$

where R_μ is the range of a muon with initial energy $E_\mu = (1 - y)E_{\nu_\mu}$ and final energy E_μ^{thr} . We assume muons lose energy continuously according to

$$\frac{dE}{dX} = -\alpha - \beta E, \quad (18)$$

where $\alpha = 2.0 \text{ MeV cm}^2/\text{g}$ and $\beta = 4.2 \times 10^{-6} \text{ cm}^2/\text{g}$ [59]. The muon range is then

$$R_\mu = \frac{1}{\beta} \ln \left[\frac{\alpha + \beta E_\mu}{\alpha + \beta E_\mu^{\text{thr}}} \right]. \quad (19)$$

In this case, $y_{\text{max}} = 1 - E_\mu^{\text{thr}}/E_\nu$ and $y_{\text{min}} = 0$.

The event rate for muons is significantly enhanced by the possibility of muons propagating from several km into the detector. Note, however, that this enhancement is θ_z -dependent: for nearly vertical down-going paths, the path length of the muon is limited by the amount of matter above the detector, not by the muon's range. This is taken into account explicitly in the simulations, and its effect will be evident in the results presented in Sec. VI.

At extremely high neutrino energies, the approximate form $P_{\text{int}} \approx R_\mu/L_{\text{SM}}^{\text{CC}}(E_{\nu_\mu})$, often presented in the literature, is less accurate than the one used here, and the difference may be significant in scenarios in which the neutrino cross section is enhanced with respect to the SM value, such as the ones we explore in this paper. Note also that in this case, our expression for P_{surv} is conservative, as it demands that the neutrino survive all the way to the detector, neglecting the possibility that it may convert a significant distance from the detector and still produce a signal.

3. *Taus*

Taus are produced only by CC ν_τ interactions. This process differs significantly from the muon case, as tau neutrinos are regenerated by tau decay through $\nu_\tau \rightarrow \tau \rightarrow \nu_\tau$ [60]. As a result, for tau neutrinos, CC and NC interactions do not deplete the ν_τ flux, but serve only to soften the neutrino energy. We include this important effect by first performing a dedicated simulation that determines $\overline{E}_{\nu_\tau}(E_{\nu_\tau}, \theta_z)$, the average energy a ν_τ has when it reaches the detector, as a function of its initial energy E_{ν_τ} and zenith angle θ_z . The tau event rate is then given by

$$N_\tau = 2\pi AT \int d\cos\theta_z \int dE_{\nu_\tau} \frac{d\Phi_{\nu_\tau}}{dE_{\nu_\tau}}(E_{\nu_\tau}) \int_{y_{\min}}^{y_{\max}} dy \frac{1}{\sigma_{\text{SM}}^{\text{CC}}(\overline{E}_{\nu_\tau})} \frac{d\sigma_{\text{SM}}^{\text{CC}}}{dy}(\overline{E}_{\nu_\tau}) \times \left[1 - \exp\left(-\frac{R_\tau((1-y)\overline{E}_{\nu_\tau})}{L_{\text{SM}}^{\text{CC}}(\overline{E}_{\nu_\tau})}\right) \right] \Theta((1-y)\overline{E}_{\nu_\tau} - E_\tau^{\text{thr}}), \quad (20)$$

where $R_\tau((1-y)\overline{E}_{\nu_\tau})$ is the range of the produced tau, but evaluated at the energy of the tau neutrino after regeneration. R_τ is given by Eq. (19) but now with $\beta = 3.6 \times 10^{-7} \text{ cm}^{-2}/\text{g}$ [59]. The last factor takes into account the requirement that the tau track be long enough to be identified in the detector. We require $E_\tau^{\text{thr}} \simeq 2.5 \times 10^6 \text{ GeV}$ so that the tau decay length is above 125 m, the string separation length in IceCube. It is not clear, at this time, whether through-going tau events will be separable from less energetic muon events. Those tau events that include one (lollipop events) or two (double bang events) showers in the detector volume will be identifiable, however. The rate of down-going lollipop events in a km^3 neutrino telescope is expected to be of the order of the rate of down-going shower events, probably slightly smaller. Double bang events will be mostly observed for neutrino energies in a limited range between roughly 10 and 100 PeV [57]. Our results assume that all tau events can be distinguished from muon events, although this may be difficult to realize.

As with muons, at very high energies taus can travel several kilometers before decaying or suffering significant energy loss. The enhancement to tau event rates from this effect is θ_z -dependent as discussed above for muons.

B. Black Hole Events

Black hole event rates may be determined with only minor modifications. For showers, the corresponding expression is

$$N_{\text{BH}} = \sum_i 2\pi AT \int d\cos\theta_z \int dE_{\nu_i} \frac{d\Phi_{\nu_i}}{dE_{\nu_i}}(E_{\nu_i}) P_{\text{surv}} \times \int_0^1 dy \frac{1}{\sigma_{\text{BH}}(E_{\nu_i})} \frac{d\sigma_{\text{BH}}}{dy}(E_{\nu_i}) P_{\text{int}} P_{\text{BH}}(E_{\nu_i}). \quad (21)$$

The survival and interaction probabilities are now

$$P_{\text{surv}} = \exp[-X(\theta_z)\sigma^{\text{tot}}(E_{\nu_i})N_A] \quad (22)$$

$$P_{\text{int}} = 1 - \exp\left[-\frac{L}{L_{\text{BH}}(E_{\nu_i})}\right], \quad (23)$$

where

$$\sigma^{\text{tot}} = \sigma_{\text{SM}}^{\text{tot}} + \sigma_{\text{BH}} , \quad (24)$$

with σ_{BH} the cross section for black hole production, and $L_{\text{BH}}(E_{\nu_i})$ is the neutrino mean free path for black hole production. As in the SM, L is the linear dimension of the detector in the case of shower events. We assume $d\sigma_{\text{BH}}/dy \propto \delta(y - 0.75)$, *i.e.*, that 75% of the black hole energy is carried away by showers, and impose that the generated shower has energy above $E_{\text{sh}}^{\text{thr}}$ to be detected. $P_{\text{BH}}(E_{\nu}) = 1$ for shower events.

In the case of muon and tau events, L is the corresponding range for the average muon or tau energy. We assume $E_{\mu,\tau} = E_{\nu}/\bar{N}$, where \bar{N} is the weighted multiplicity discussed in Eq. (11). The true $E_{\mu,\tau}$ distribution is essentially flat with endpoints 0 and $2E_{\nu}/\bar{N}$. Our simplification is valid except for lepton energies near threshold. In addition, spreading the lepton energy has two compensating effects, as some leptons below threshold become detectable, and some above threshold drop below threshold. We have checked that the error made is insignificant at the $\sim 10\%$ level.

To account for the branching fraction to leptons, we include

$$P_{\text{BH}}(E_{\nu_i}) = 1 - \exp \left[-\frac{\bar{N}(E_{\nu_i})}{30} \right] , \quad (25)$$

the probability of obtaining at least one muon (or tau) in the decay of a black hole when the expected muon (or tau) multiplicity is $\bar{N}/30$.

V. RATES

The integrated event rates for showers, muons, and taus are shown in Tables I, II, and III, respectively. We consider IceCube, with a representative depth of 1.8 km. We give results for various n , M_D , x_{min} , and with and without exponential suppression in the parton cross section. Only down-going rates are presented. Up-going rates are, as expected, extremely suppressed in the presence of black hole production, as will be seen in Sec. VI.

For showers, the geometric cross section $\hat{\sigma} = \pi r_s^2$, and $M_D = 1$ TeV, we find a few events per year in each channel for cosmogenic fluxes, and as many as tens of events per year for the WB flux. These event rates are far above SM background. For the WB flux, bounds from AGASA and Fly's Eye will imply limits above $M_D = 1$ TeV, but even for $M_D = 2$ TeV, we find reasonable rates. In this case, however, the SM background will be important. For the exponentially suppressed parton cross section, event rates are suppressed, but not drastically so. In fact, for $x_{\text{min}} = 1$, $\sim \mathcal{O}(1)$ event per year is possible given the cosmogenic flux. For $x_{\text{min}} = 3$, the exponential suppression is large, and event rates are highly suppressed.

Generally, event rates are on more solid footing for larger x_{min} , where both the semi-classical production cross section and the assumption of thermal decay are more reliable. For showers, however, our event rate calculation relies essentially only on the requirement that black holes decay to visible showers and is insensitive to the details of evaporation. At the same time, while the production cross section for black holes (or their stringy Planck mass progenitors [42]) is subject to significant quantum corrections for $M_{\text{BH}} \approx M_D$, there is no reason to expect it to vanish or be greatly suppressed. For showers, then, we find the requirement $x_{\text{min}} = 1$ reasonable.

Qualitatively similar conclusions apply for muons and taus. While these event rates are suppressed relative to shower rates by the branching ratio for black hole decay to leptons,

TABLE I: Event rate for down-going showers (in 2π sr) with $E_{\text{sh}}^{\text{thr}} = 500$ TeV in IceCube. We consider the Waxman-Bahcall [51] and cosmogenic [46] fluxes, $M_D = 1$ and 2 TeV, and various cases $(n, x_{\text{min}}, \hat{\sigma})$, where n is the number of extra dimensions, $x_{\text{min}} \equiv M_{\text{BH}}^{\text{min}}/M_D$, and $\hat{\sigma}$ is the parton level cross section for black hole production.

Showers ($\text{km}^{-3} \text{ yr}^{-1}$)	WB Flux		Cosmogenic Flux	
	$M_D = 1$ TeV	$M_D = 2$ TeV	$M_D = 1$ TeV	$M_D = 2$ TeV
Standard Model	4.8	4.8	0.1	0.1
BH (6, 1, πr_s^2)	44.6	3.1	5.2	0.9
BH (6, 3, πr_s^2)	6.5	0.5	2.3	0.3
BH (6, 1, $\pi r_s^2 e^{-I}$)	18.5	1.2	2.1	0.3
BH (6, 3, $\pi r_s^2 e^{-I}$)	0.4	2.8×10^{-2}	0.1	1.5×10^{-2}
BH (3, 1, πr_s^2)	16.3	1.1	2.7	0.4
BH (3, 3, πr_s^2)	3.0	0.2	1.2	0.1
BH (3, 1, $\pi r_s^2 e^{-I}$)	3.8	0.2	0.5	6.1×10^{-2}
BH (3, 3, $\pi r_s^2 e^{-I}$)	2.9×10^{-2}	1.9×10^{-3}	8.6×10^{-3}	9.3×10^{-4}

TABLE II: As in Table I, but for the flux of down-going muons and $E_{\mu}^{\text{thr}} = 500$ TeV.

Muons ($\text{km}^{-2} \text{ yr}^{-1}$)	WB Flux		Cosmogenic Flux	
	$M_D = 1$ TeV	$M_D = 2$ TeV	$M_D = 1$ TeV	$M_D = 2$ TeV
Standard Model	6.0	6.0	0.2	0.2
BH (6, 1, πr_s^2)	27.7	2.6	4.9	1.1
BH (6, 3, πr_s^2)	12.0	1.1	4.9	0.7
BH (6, 1, $\pi r_s^2 e^{-I}$)	8.8	0.7	1.3	0.2
BH (6, 3, $\pi r_s^2 e^{-I}$)	0.6	4.6×10^{-2}	0.2	2.5×10^{-2}
BH (3, 1, πr_s^2)	14.0	1.2	4.2	0.6
BH (3, 3, πr_s^2)	7.1	0.6	3.5	0.4
BH (3, 1, $\pi r_s^2 e^{-I}$)	1.8	0.1	0.3	4.1×10^{-2}
BH (3, 3, $\pi r_s^2 e^{-I}$)	4.2×10^{-2}	3.1×10^{-3}	1.5×10^{-2}	1.6×10^{-3}

TABLE III: As in Table I, but for the flux of down-going taus and $E_{\tau}^{\text{thr}} = 2.5 \times 10^6$ GeV.

Taus ($\text{km}^{-2} \text{ yr}^{-1}$)	WB Flux		Cosmogenic Flux	
	$M_D = 1$ TeV	$M_D = 2$ TeV	$M_D = 1$ TeV	$M_D = 2$ TeV
Standard Model	0.9	0.9	0.1	0.1
BH (6, 1, πr_s^2)	15.1	2.2	5.0	1.2
BH (6, 3, πr_s^2)	7.7	1.0	4.5	0.7
BH (6, 1, $\pi r_s^2 e^{-I}$)	4.5	0.6	1.3	0.2
BH (6, 3, $\pi r_s^2 e^{-I}$)	0.5	4.4×10^{-2}	0.2	2.9×10^{-2}
BH (3, 1, πr_s^2)	8.7	1.1	4.1	0.7
BH (3, 3, πr_s^2)	4.8	0.6	3.1	0.4
BH (3, 1, $\pi r_s^2 e^{-I}$)	1.0	0.1	0.4	5.2×10^{-2}
BH (3, 3, $\pi r_s^2 e^{-I}$)	2.9×10^{-2}	2.8×10^{-3}	1.6×10^{-2}	1.8×10^{-3}

they are enhanced by the possibility of muons and taus propagating from many km away into the detector. We find that these effects effectively balance each other. In the case of muons and taus, we have assumed thermal decay distributions, which may not be accurate for $x_{\min} \approx 1$. The event rates are hardly reduced for $x_{\min} = 3$, however; as noted in Sec. II, the more stringent x_{\min} requirement preferentially eliminates events with low multiplicities, and so has little impact on lepton rates.

The muon flux is significantly larger for the WB flux than for the cosmogenic flux. This is straightforward to understand — the WB flux is larger at low energies. The tau event rate is not as greatly enhanced, however. The tau decay length is 4.9 km ($E_\tau/10^8$ GeV). While the WB flux enhances fluxes at low energies, the resulting taus decay before they lose energy, and the tau range is therefore diminished. Larger low energy fluxes therefore do not enhance the tau rate as significantly.

In addition to enhancing the SM event rates by more than an order of magnitude, Tables I-III show that black hole production may also change the relative event rates of the various channels. The ability of neutrino telescopes, unique among cosmic ray experiments, to differentiate showers, muons, and possibly taus, allows one to measure these relative event rates. Given sufficient statistics, this may provide an important signal of physics beyond the SM.

VI. ANGLE AND ENERGY DISTRIBUTIONS

Neutrino telescopes may also measure angle and energy distributions, providing additional opportunities to distinguish black hole events from SM or other possible physics and for constraining black hole properties.

The zenith angle distributions of SM and black hole events for showers, muons, and taus are given in Figs. 4, 5, and 6, respectively. Black hole production makes the Earth even more opaque to ultra-high energy neutrinos, reducing the up-going rate, while increasing the probability of interaction, and thereby the event rate, of down-going neutrinos. In all cases, up-going events rates are below SM contributions. No sensitivity to black hole production is then expected when looking for up-going events.

The characteristic features of the zenith angle distribution of showers compared to the distributions of muons and taus are also noteworthy. For showers, vertical fluxes are less attenuated than horizontal ones, and so the angular distribution is maximized for vertically down-going events. In contrast, as noted in Sec. IV A, vertically down-going muon and tau events cannot benefit from muon and tau ranges beyond the depth of the detector (~ 2 km). The optimal direction for muon and tau events is therefore closer to the horizon. In scenarios with enhanced cross sections such as the one we are exploring in this paper, the neutrino flux is attenuated even in the horizontal direction as can be seen in Figs. 5 and 6. As a consequence, the quasi-horizontal direction with small but positive $\cos\theta_z$, where the effects of attenuation are maximally offset by lepton range, leads to the largest rates. For muons, this optimal zenith angle is around $\cos\theta_z \approx 0.2$. For taus, with even longer ranges, it is $\cos\theta_z \approx 0.4$. These are general considerations that apply to the detection of ultra-high energy neutrinos in any scenario predicting enhanced cross sections with respect to the SM cross sections.

Energy distributions for the various channels are given in Figs. 7, 8, and 9. The energy distributions are clearly sensitive to x_{\min} and the presence or absence of exponential suppression in the parton cross section. Different types of events therefore probe different

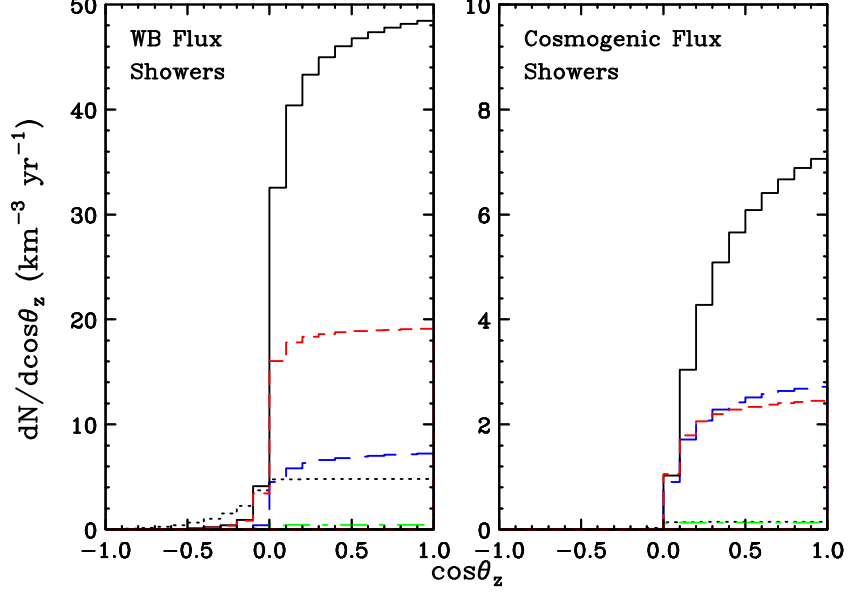


FIG. 4: Zenith angle distribution of shower events for $M_D = 1$ TeV, $E_{\text{sh}}^{\text{thr}} = 500$ TeV, and $(n, x_{\text{min}}, \hat{\sigma}) = (6, 1, \pi r_s^2)$ (solid), $(6, 3, \pi r_s^2)$ (long dash), $(6, 1, \pi r_s^2 e^{-I})$ (short dash), $(6, 3, \pi r_s^2 e^{-I})$ (dot-dash). Also shown is the standard model prediction (dotted).

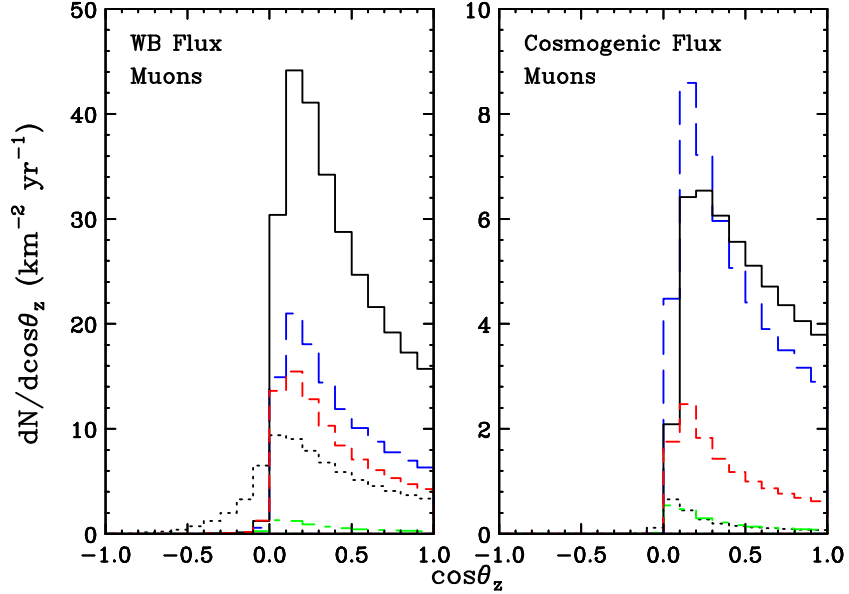


FIG. 5: As in Fig. 4, but for muon events with $E_{\mu}^{\text{thr}} = 500$ TeV.

and complementary aspects of black hole production and decay. By measuring the down-going energy distributions with reasonable statistics, the IceCube detector may be able to discriminate between the different possibilities. Note that to facilitate comparison with conventional presentations of SM rates at neutrino telescopes, we have plotted distributions in initial neutrino energy. Shower energies are related to these neutrino energies in a fairly direct way, and the shower energy distributions will have roughly the same shape. The energy

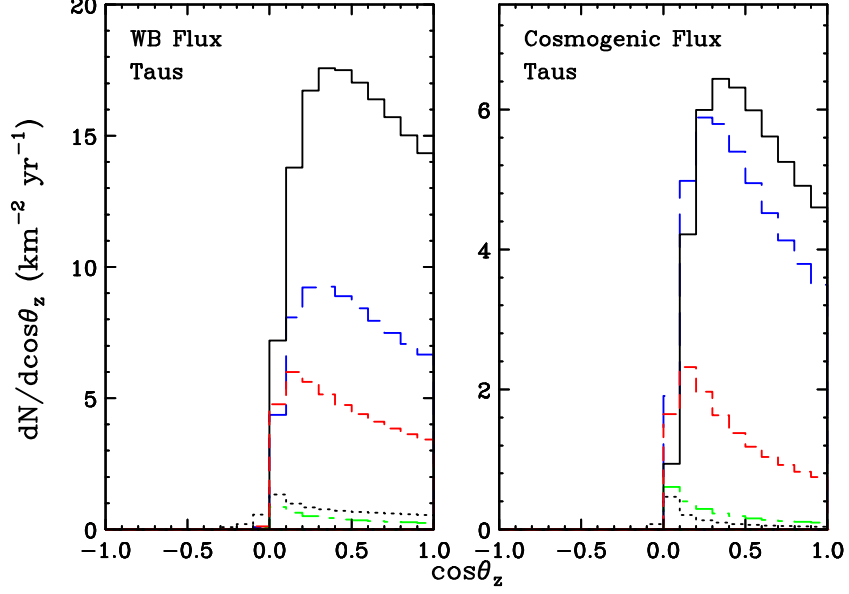


FIG. 6: As in Fig. 4, but for tau events with $E_7^{\text{thr}} = 2.5 \times 10^6$ GeV.

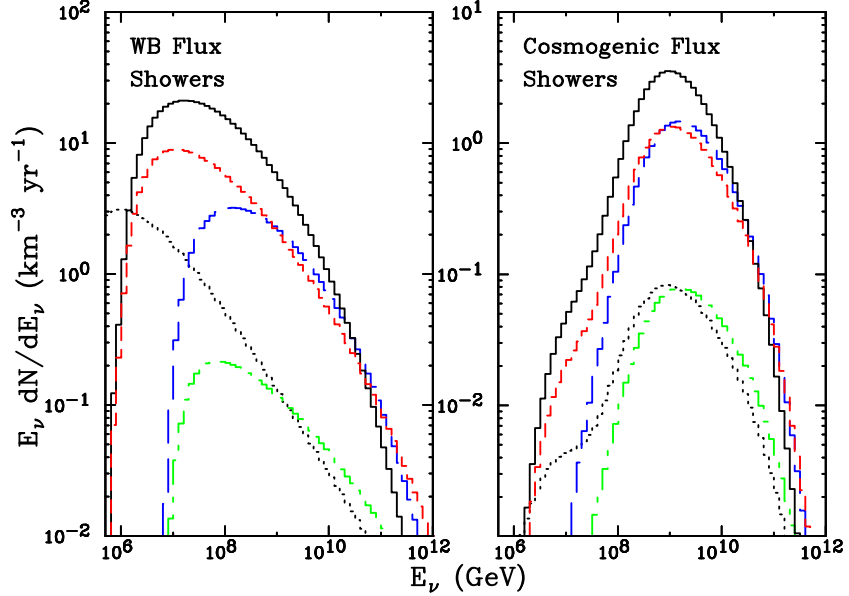


FIG. 7: Energy distribution of down-going shower events for $M_D = 1$ TeV, $E_{\text{sh}}^{\text{thr}} = 500$ TeV, and $(n, x_{\text{min}}, \hat{\sigma}) = (6, 1, \pi r_s^2)$ (solid), $(6, 3, \pi r_s^2)$ (long dash), $(6, 1, \pi r_s^2 e^{-I})$ (short dash), $(6, 3, \pi r_s^2 e^{-I})$ (dot dash). Also shown is the standard model prediction (dotted).

distributions of through-going leptons may be significantly distorted, however, as the lepton energy is a function of black hole multiplicity as well as the distance the lepton propagates before reaching the detector. Note also that, while shower energies should be well-measured, lepton energy measurements present significant challenges, especially for taus. Lollipop tau events will be a clear tau signature with well-measured energy. However, determining the energy of through-going tau events will be difficult in IceCube as they typically do not ra-

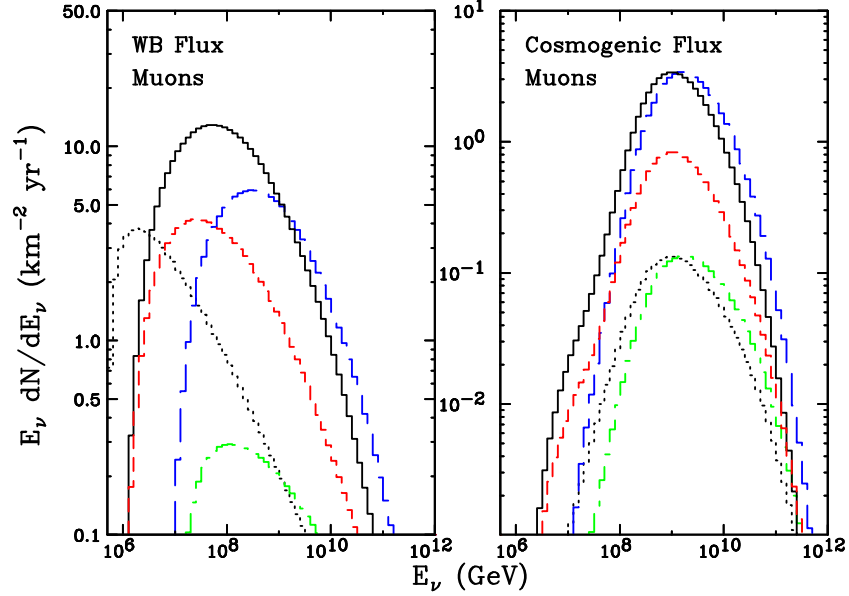


FIG. 8: As in Fig. 7, but for down-going muon events with $E_\mu^{\text{thr}} = 500$ TeV.

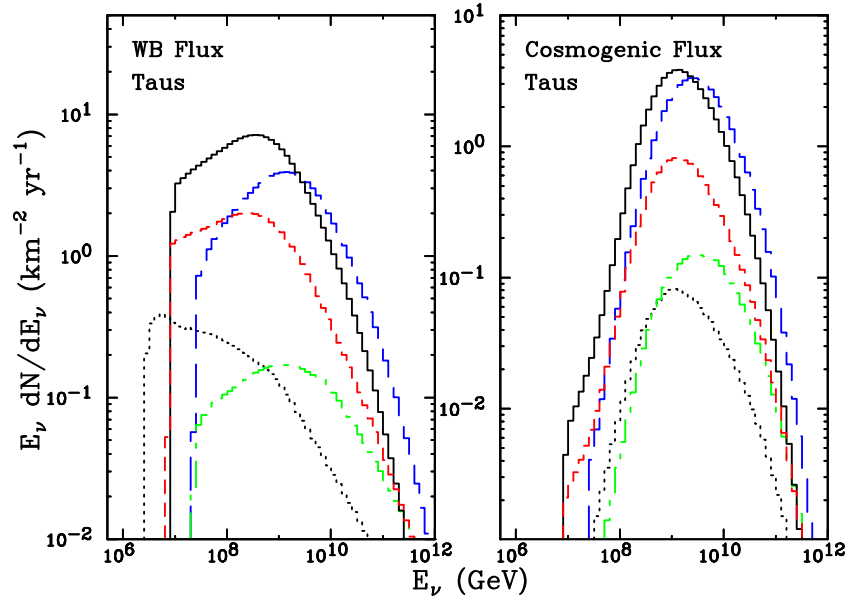


FIG. 9: As in Fig. 7, but for down-going tau events with $E_\tau^{\text{thr}} = 2.5 \times 10^6$ GeV.

diate and, therefore, appear similar to minimum ionizing muons with energy ~ 200 GeV. More detailed detector simulations will be necessary to effectively use the information from through-going taus described in this paper.

VII. PROSPECTS AND CONCLUSIONS

In the presence of TeV-scale gravity and extra dimensions, ultra-high energy cosmic neutrinos may produce microscopic black holes in the surface of the Earth. We have explored

the prospects for detecting such events in neutrino telescopes. We considered contained showers, through-going muons, and also through-going taus.

The rates for a km^3 detector, such as IceCube, are of the order of a few per year in each channel for M_D near current bounds. These rates are well above SM backgrounds, and provide a significant opportunity to observe black hole production. In several years of data taking at a kilometer-scale neutrino telescope, it should be possible to probe most of the cases described in this paper: values of M_D well above 1 TeV may be within reach, and observable event rates are even possible for exponentially suppressed parton cross sections. At the same time, these results imply that black hole observation at ANTARES and NESTOR appears unlikely, given their effective areas of $\lesssim 0.1 \text{ km}^2$. The RICE experiment [61], which aims to detect coherent Cerenkov radiation from electromagnetic and hadronic showers at frequencies of 100 MHz to 1 GHz, provides another interesting and complementary probe with effective volume for shower detection reaching $\sim 1 \text{ km}^3$ above a few PeV.

The expected rates for black hole events are, of course, highly sensitive to the choice of neutrino flux. As this work was being completed, a paper also discussing black holes at neutrino telescopes appeared [26]. There, results for two fluxes are presented: a “limit from hidden sources” flux and a cosmogenic flux. The first flux is roughly 3 times higher than the limit placed by the AMANDA experiment on diffuse fluxes [62]. The WB flux we use is much more conservative and is roughly 2 orders of magnitude smaller. A variety of cosmogenic fluxes [63, 64] are also considered in Ref. [26]. Our ratios of black hole to SM rates are in agreement, but here, too, it appears we have chosen a more conservative representative flux, leading to a factor of 3 to 5 fewer shower and muon events from cosmogenic neutrinos. The possibility of tau events, exponentially suppressed cross sections, and angle and energy distributions were not addressed in Ref. [26].

Relative to IceCube, the prospects for black hole detection appear to be slightly brighter at the Auger Observatory, expected to be completed by 2004, where tens of events per year may be discovered [11, 14, 15]. IceCube is scheduled to reach its ultimate goal of 1 km^3 in 2009, but it will collect data continuously as it grows in stages, beginning with the existing AMANDA II detector, roughly of area 0.1 km^2 , and reaching a volume of around 0.5 km^3 in 2006. It is difficult to model this time-varying detection volume, but by 2007, an integrated exposure of roughly $1 \text{ km}^3 \text{ yr}$ will have been achieved. Given the rates of Tables I-III, we conclude that, for scenarios with M_D near current bounds, IceCube may detect black hole events along with the Auger Observatory before the LHC begins operation.

Of course, enhanced event rates alone are not necessarily a signal of new physics. In particular, the uncertainty of astrophysical neutrino fluxes makes it difficult to determine whether observed events result from the SM or new physics based on counting experiments alone. Comparisons of quasi-horizontal showers and Earth-skimming neutrino rates provide a powerful discriminant in ground arrays [11, 15]. However, the possibility of measuring relative event rates in three separate channels at IceCube provides a direct, unique, and complementary tool for distinguishing black hole events from the SM and other new physics possibilities. As noted in Sec. VI, angular and energy distributions will also be helpful to separate the signal of a large astrophysical flux from the signal of new physics. The separation of these channels in ground arrays and fluorescence detectors is extremely difficult.

Given sufficient statistics, then, the information provided by IceCube may provide information on black hole branching ratios, and the various angle and energy distributions may also help distinguish various properties of black hole production and decay. Black hole production may be the best prospect for discovering extra dimensions in the near future,

and neutrino telescopes may be an excellent tool for studying them.

Acknowledgments

We thank Gonzalo Parente for invaluable help with implementing the CTEQ parton distribution functions in our simulation, Ralph Engel for providing the cosmogenic neutrino flux, and Alfred Shapere for helpful conversations. J.A.-M. is supported by NASA Grant NAG5-7009. The work of J.L.F. was supported in part by the Department of Energy under cooperative research agreement DF-FC02-94ER40818. This work was supported in part by DOE grant No. DE-FG02-95ER40896 and in part by the Wisconsin Alumni Research Foundation.

-
- [1] I. Antoniadis, N. Arkani-Hamed, S. Dimopoulos and G. Dvali, Phys. Lett. B **436**, 257 (1998) [hep-ph/9804398].
 - [2] D. Amati, M. Ciafaloni and G. Veneziano, Phys. Lett. B **197**, 81 (1987); Phys. Lett. B **289**, 87 (1992).
 - [3] G. 't Hooft, Phys. Lett. B **198**, 61 (1987); Commun. Math. Phys. **117**, 685 (1988).
 - [4] P. C. Argyres, S. Dimopoulos and J. March-Russell, Phys. Lett. B **441**, 96 (1998) [hep-th/9808138].
 - [5] T. Banks and W. Fischler, hep-th/9906038.
 - [6] R. Emparan, G. T. Horowitz and R. C. Myers, Phys. Rev. Lett. **85**, 499 (2000), hep-th/0003118.
 - [7] S. B. Giddings and E. Katz, J. Math. Phys. **42**, 3082 (2001) [hep-th/0009176].
 - [8] S. B. Giddings and S. Thomas, hep-ph/0106219.
 - [9] S. Dimopoulos and G. Landsberg, Phys. Rev. Lett. **87**, 161602 (2001) [hep-ph/0106295].
 - [10] S. W. Hawking, Commun. Math. Phys. **43**, 199 (1975).
 - [11] J. L. Feng and A. D. Shapere, Phys. Rev. Lett. **88**, 021303 (2002) [hep-ph/0109106].
 - [12] L. Anchordoqui and H. Goldberg, Phys. Rev. D **65**, 047502 (2002) [hep-ph/0109242].
 - [13] R. Emparan, M. Masip and R. Rattazzi, hep-ph/0109287.
 - [14] A. Ringwald and H. Tu, Phys. Lett. B **525**, 135 (2002) [hep-ph/0111042].
 - [15] L. A. Anchordoqui, J. L. Feng, H. Goldberg and A. D. Shapere, hep-ph/0112247.
 - [16] X. Bertou, P. Billoir, O. Deligny, C. Lachaud and A. Letessier-Selvon, astro-ph/0104452.
 - [17] J. L. Feng, P. Fisher, F. Wilczek and T. M. Yu, hep-ph/0105067.
 - [18] A. Kusenko and T. Weiler, hep-ph/0106071.
 - [19] R. M. Baltrusaitis *et al.*, Phys. Rev. D **31**, 2192 (1985).
 - [20] S. Yoshida *et al.* [AGASA Collaboration], in *Proc. 27th International Cosmic Ray Conference*, Hamburg, Germany, 2001, Vol. 3, p. 1142.
 - [21] E. J. Ahn, M. Cavaglia and A. V. Olinto, hep-th/0201042.
 - [22] P. Jain, S. Kar, S. Panda and J. P. Ralston, hep-ph/0201232.
 - [23] <http://www.ssec.wisc.edu/a3ri/icecube>.
 - [24] ANTARES Collaboration, J. R. Hubbard *et al.*, HE.6.3.03 and ANTARES Collaboration, L. Moscoso *et al.*, HE.6.3.04 in *Proceedings of the 26th International*

- Cosmic Ray Conference (ICRC 99)*, Salt Lake City, Utah, 17-25 August 1999, <http://krusty.physics.utah.edu/~icrc1999/proceedings.html>.
- [25] NESTOR Collaboration, L. K. Resvanis *et al.*, talk given at the 8th International Workshop on Neutrino Telescopes, Venice, Italy, 23-26 February 1999.
 - [26] M. Kowalski, A. Ringwald and H. Tu, hep-ph/0201139.
 - [27] Y. Uehara, hep-ph/0110382.
 - [28] M. B. Voloshin, Phys. Lett. B **518**, 137 (2001) [hep-ph/0107119].
 - [29] M. B. Voloshin, Phys. Lett. B **524**, 376 (2002) [hep-ph/0111099].
 - [30] S. Nussinov and R. Shrock, Phys. Rev. D **59**, 105002 (1999) [hep-ph/9811323].
 - [31] P. Jain, D. W. McKay, S. Panda and J. P. Ralston, Phys. Lett. B **484**, 267 (2000) [hep-ph/0001031].
 - [32] C. Tyler, A. V. Olinto and G. Sigl, Phys. Rev. D **63**, 055001 (2001) [hep-ph/0002257].
 - [33] J. Alvarez-Muniz, F. Halzen, T. Han and D. Hooper, Phys. Rev. Lett. **88**, 021301 (2002) [hep-ph/0107057].
 - [34] S. Cullen and M. Perelstein, Phys. Rev. Lett. **83**, 268 (1999) [hep-ph/9903422]; V. Barger, T. Han, C. Kao and R. J. Zhang, Phys. Lett. B **461**, 34 (1999) [hep-ph/9905474]; L. J. Hall and D. R. Smith, Phys. Rev. D **60**, 085008 (1999) [hep-ph/9904267]; C. Hanhart, J. A. Pons, D. R. Phillips and S. Reddy, Phys. Lett. B **509**, 1 (2001) [astro-ph/0102063]; S. Hannestad and G. Raffelt, Phys. Rev. Lett. **87**, 051301 (2001) [hep-ph/0103201]; S. Hannestad and G. G. Raffelt, hep-ph/0110067.
 - [35] G. F. Giudice, R. Rattazzi and J. D. Wells, Nucl. Phys. B **544**, 3 (1999) [hep-ph/9811291]; E. A. Mirabelli, M. Perelstein and M. E. Peskin, Phys. Rev. Lett. **82**, 2236 (1999) [hep-ph/9811337]; T. Han, J. D. Lykken and R. J. Zhang, Phys. Rev. D **59**, 105006 (1999) [hep-ph/9811350]; J. L. Hewett, Phys. Rev. Lett. **82**, 4765 (1999) [hep-ph/9811356]; T. G. Rizzo, Phys. Rev. D **59**, 115010 (1999) [hep-ph/9901209].
 - [36] For a summary of LEP bounds, see C. Pagliarone, hep-ex/0111063.
 - [37] B. Abbott *et al.* [D0 Collaboration], Phys. Rev. Lett. **86**, 1156 (2001) [hep-ex/0008065].
 - [38] R. C. Myers and M. J. Perry, Annals Phys. **172**, 304 (1986).
 - [39] P. D. D'Eath and P. N. Payne, Phys. Rev. D **46**, 658 (1992); Phys. Rev. D **46**, 675 (1992); Phys. Rev. D **46**, 694 (1992).
 - [40] D. M. Eardley and S. B. Giddings, gr-qc/0201034.
 - [41] S. N. Solodukhin, hep-ph/0201248.
 - [42] S. Dimopoulos and R. Emparan, hep-ph/0108060.
 - [43] S. B. Giddings, hep-ph/0110127.
 - [44] H. L. Lai *et al.* [CTEQ Collaboration], Eur. Phys. J. C **12**, 375 (2000) [hep-ph/9903282].
 - [45] F. W. Stecker, Astrophys. J. **228**, 919 (1979).
 - [46] R. Engel, D. Seckel and T. Stanev, Phys. Rev. D **64**, 093010 (2001) [astro-ph/0101216].
 - [47] E. Waxman and J. N. Bahcall, Phys. Rev. Lett. **78**, 2292 (1997) [astro-ph/9701231].
 - [48] E. Waxman, astro-ph/0103186.
 - [49] F. Halzen and D. W. Hooper, Astrophys. J. **527**, L93 (1999) [astro-ph/9908138].
 - [50] J. Alvarez-Muniz, F. Halzen and D. W. Hooper, Phys. Rev. D **62**, 093015 (2000) [astro-ph/0006027].
 - [51] E. Waxman and J. N. Bahcall, Phys. Rev. D **59**, 023002 (1999) [hep-ph/9807282]; J. N. Bahcall and E. Waxman, Phys. Rev. D **64**, 023002 (2001) [hep-ph/9902383].
 - [52] F. Halzen and D. Hooper, hep-ph/0110201.
 - [53] S. Sarkar and R. Toldra, Nucl. Phys. B **621**, 495 (2002) [hep-ph/0108098].

- [54] M. Birkel and S. Sarkar, *Astropart. Phys.* **9**, 297 (1998) [hep-ph/9804285].
- [55] V. Berezhinsky, M. Kachelriess and A. Vilenkin, *Phys. Rev. Lett.* **79**, 4302 (1997) [astro-ph/9708217].
- [56] H. Athar, M. Jezabek and O. Yasuda, *Phys. Rev. D* **62**, 103007 (2000) [hep-ph/0005104].
- [57] <http://www.ssec.wisc.edu/a3ri/icecube/public/nutau.pdf>.
- [58] A. Dziewonski, “Earth Structure, Global,” in *The Encyclopedia of Solid Earth Geophysics*, edited by D. E. James (Van Nostrand Reinhold, New York, 1989), p. 331.
- [59] S. I. Dutta, M. H. Reno, I. Sarcevic and D. Seckel, hep-ph/0012350.
- [60] F. Halzen and D. Saltzberg, *Phys. Rev. Lett.* **81**, 4305 (1998) [hep-ph/9804354].
- [61] I. Kravchenko *et al.* [RICE Collaboration], astro-ph/0112372.
- [62] E. Andres *et al.*, *Nature* **410**, 441 (2001).
- [63] S. Yoshida and M. Teshima, *Prog. Theor. Phys.* **89**, 833 (1993).
- [64] R. J. Protheroe and P. A. Johnson, *Astropart. Phys.* **4**, 253 (1996) [astro-ph/9506119].